Temperature stability of field induced anisotropy in soft ferromagnetic Fe,Co-based amorphous and nanocomposite ribbons

P. R. Ohodnicki,[1,2,a)] D. E. Laughlin,[1,2] M. E. McHenry,[1] V. Keylin,[1,2] and J. Huth[2]

[1]*Department of Materials Science and Engineering, Carnegie Mellon University, Pittsburgh, Pennsylvania 15213, USA*

[2]*Magnetics, Division of Spang and Company, Pittsburgh, Pennsylvania 15238, USA*

The temperature stability of field induced uniaxial anisotropy (K_U) was investigated by thermomagnetic treatments of $(Co_{1-x}Fe_x)_{89}Zr_7B_4$ amorphous ribbons after field annealing below and above the crystallization temperature. We conclude: (1) Field annealing treatments are necessary to properly investigate the temperature stability of K_U, (2) K_U of field crystallized alloys exhibit improved temperature stability relative to alloys remaining amorphous after field annealing, and (3) larger K_U is obtained for field crystallization treatments as compared to zero-field crystallization followed by field reannealing. Field crystallization may be required for elevated temperature applications when field induced anisotropy is critical for performance. © *2009 American Institute of Physics*. [DOI: 10.1063/1.3068547]

Magnetic field annealing[1,2] is used to tailor magnetic properties of soft magnetic materials by inducing a uniaxial magnetic anisotropy energy, K_U. The induced easy axis can be controlled by applying a saturating magnetic field (i.e., field annealing). However, induced anisotropy due to "self-field annealing"[2] also develops in the absence of an external field resulting in a spatially varying distribution of induced anisotropies that stabilize the remanent domain structure of the material. Field annealing treatments are particularly important for soft ferromagnetic Fe,Co-based amorphous and nanocomposite alloys. The effective magnetocrystalline anisotropy is greatly reduced by exchange coupling of regions with rapid spatial variations (over $\sim 10^{-10}$–10^{-9} m) of local easy axis orientations.[3] K_U due to induced magnetic anisotropies can dominate the effective magnetocrystalline anisotropy because of greater spatial coherency.[4–6]

Toroidal tape wound cores of amorphous or nanocomposite ribbons can be annealed in a longitudinal or a transverse saturating field. Large K_U is often undesirable for zero or longitudinally field annealed cores as it can dominate the effective magnetic anisotropy and result in large hysteretic losses due to domain wall pinning.[4] However, for transverse field annealed cores large K_U can be desirable resulting in higher saturation fields, lower permeabilities, and improved high frequency response.[7,8]

K_U in Fe,Co-based soft magnetic amorphous and amorphous/nanocrystalline "nanocomposite" alloy systems has been reported and discussed in a number of previous works.[5–12] Co-rich nanocomposites tend to exhibit relatively large values of K_U as compared to the corresponding Fe-rich compositions. (Fe,Co)–Zr–B is one of the most widely studied alloy systems due to high saturation magnetizations and Curie temperatures. We have previously reported the compositional dependence of K_U for transverse field annealed $(Co_{1-x}Fe_x)_{89}Zr_7B_4$ and $(Co_{1-x}Fe_x)_{88}Zr_7B_4Cu_1$.[9,10] In this work, we discuss the temperature stability of K_U using subsequent thermomagnetic treatments of selected ribbons from our previous reports. The ribbons were initially field annealed at temperatures above or below the primary crystallization temperature, $T_{x1} \sim 450$ °C. Emphasis is placed on the $(Co_{0.975}Fe_{0.025})_{89}Zr_7B_4$ composition for which a large value of K_U ($\sim 20\,000$–$25\,000$ ergs/cm^3) was observed after field crystallization to produce BCC, FCC, and HCP nanocrystals surrounded by an intergranular amorphous phase.[9,10,13] Results are also discussed for alloys with varying Fe, Co content and the $(Co_{0.88}Fe_{0.12})_{79.4}Nb_{2.6}Si_9B_9$ composition investigated by other authors.[11,12]

Amorphous ribbons were synthesized by arc-melting and single roller wheel melt spinning. Toroidal wound cores were annealed in flowing N_2 for 1 h with a 2 T transverse field. The cores were then reannealed with or without a longitudinal applied saturating field of $H > 50$ Oe under flowing N_2. Dynamic B-H loops at $f = 3$ kHz were measured using ac permeametry to estimate the anisotropy field, H_K, by extrapolating the low-field linear portion of the B-H loop to saturation. The room temperature saturation magnetization, M_S, was measured by vibrating sample magnetometry. H_K and M_S were used to estimate the value of K_U using the expression $K_U = (H_K M_S)/2$. Phase identification and microstructural investigations are discussed in detail elsewhere.[9,10,13]

A dramatic difference in the temperature stability of K_U was observed for zero field and longitudinal field reannealing of initially transverse field annealed ribbons. This is illustrated in Fig. 1 for a $(Co_{0.975}Fe_{0.025})_{89}Zr_7B_4$ alloy after a $T_{anneal} = 350$ °C transverse field annealing treatment (field annealed amorphous). Figure 1(a) shows measured values of H_K at room temperature after reannealing the sample at increasing temperatures for 1 h. Because M_S of the as-cast and

a)Author to whom correspondence should be addressed. Electronic mailpaul.ohodnicki@gmail.com.
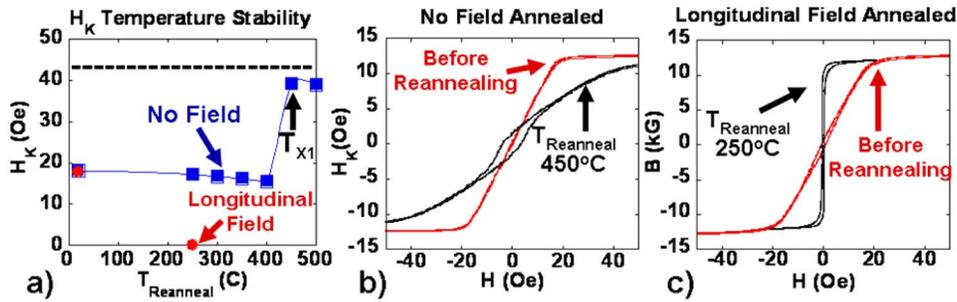
FIG. 1. (Color online) (a) H_K measured at room temperature vs reannealing temperature with and without a longitudinal applied field of $H > \sim 50$ Oe for initially transverse field annealed amorphous ($T_{anneal} = 350$ °C) toroidal $(Fe_{0.025}Co_{0.975})_{89}Zr_7B_4$ cores. The dashed line is the measured H_K for a transverse field crystallized alloy for comparison ($T_{anneal} = 540$ °C). Representative B-H loops for the (b) zero-field reannealed and (c) longitudinal field reannealed samples. In (a) T_{X1} is the reannealing temperature at which the initially amorphous ribbon crystallizes to form a nanocomposite.

crystallized ribbons are almost identical for this composition,[9,10] the trend in H_K of Fig. 1 also illustrates the trend in K_U. For zero-field reannealing treatments, the initial values of $H_K \sim 18$ Oe and $K_U \sim 8400$ ergs/cm^3 decrease slightly with increasing reannealing temperatures. An increase occurs upon reannealing at temperatures sufficiently high for crystallization to occur due to the larger values of H_K and K_U for field crystallized alloys of this composition.[9,10] This observation demonstrates that the zero-field reannealing treatments are effectively a "self-transverse field anneal" due to the high Curie temperature of the as-cast amorphous ribbon and a transverse remanent domain structure established by the initial transverse field anneal.

Measured B-H loops after the initial transverse field annealing and after zero-field reannealing up to 450 °C to result in crystallization are presented in Fig. 1(b). The B-H loops are less linear for such "self-transverse field crystallized" alloys as compared to alloys crystallized in a transverse, saturating external field [e.g., Fig. 2(a)] presumably due to the more complex induced anisotropy distribution (e.g., in the vicinity of domain walls). For comparison, the B-H loops are also presented for an initially transverse field annealed amorphous ribbon before and after longitudinal

field reannealing at $T_{reanneal} = 250$ °C in Fig. 1(c). The transverse field induced anisotropy is completely eliminated even at this low annealing temperature demonstrating that "self-field annealing" effects must be avoided by applying a saturating longitudinal or rotating[4] magnetic field to properly investigate the temperature stability of K_U through reannealing treatments. Therefore we subsequently focus only on results obtained for longitudinal field reannealing treatments.

Figure 2 shows the results of longitudinal field reannealing treatments for the high K_U compositions ($Co_{0.975}Fe_{0.025})_{89}Zr_7B_4$ [Fig. 2(a)] and $(Co_{0.88}Fe_{0.12})_{79.4}Nb_{2.6}Si_9B_9$ [Fig. 2(b)] after transverse field crystallization at $T_{anneal} = 540$ °C. For the field crystallized alloys, M_S does not change significantly during reannealing and so H_K again represents the trend in K_U. Both field crystallized alloys exhibit improved temperature stability as compared to the field annealed amorphous alloy of Fig. 1 for which measurable values of H_K were eliminated after a longitudinal field reannealing treatment at temperatures as low as $T_{reanneal} = 250$ °C. A difference in temperature stability can potentially be explained by a higher atomic mobility in the as-cast amorphous ribbons.[2] For the $(Co_{0.88}Fe_{0.12})_{79.4}Nb_{2.6}Si_9B_9$ alloy, the B-H loops exhibit a "kink" after longitudinal field reannealing so the estimates of H_K are a slight, but consistent, overestimate of the field at which the core saturates.

A correlation between H_K and coercivity (H_C) is not observed for the $(Co_{0.975}Fe_{0.025})_{89}Zr_7B_4$ alloy [Fig. 2(c)] but a rough correlation is observed for the $(Co_{0.88}Fe_{0.12})_{79.4}Nb_{2.6}Si_9B_9$ alloy [Fig. 2(d)]. A correlation between H_K and static values of H_C would be reasonable in the framework of the extended random anisotropy model where K_U dominates the overall effective anisotropy.[5,6] However, we cannot address this issue here as the measured values of H_C are dynamic and there is some ambiguity in using this model to explain the coercivities of transverse field annealed cores where magnetization occurs primarily through rotation.

In Fig. 3(a), H_K is presented as a function of longitudinal field reannealing temperature for several different alloys. Figure 3(b) demonstrates the total reduction in H_K after reannealing treatments for 1 h while Fig. 3(c) presents the fractional reduction in H_K. These results illustrate that, with the exception of the $x = 0.15$ alloy, all of the field crystallized ribbons exhibit enhanced temperature stability of K_U as compared to the field annealed amorphous ribbon of Fig. 1. The
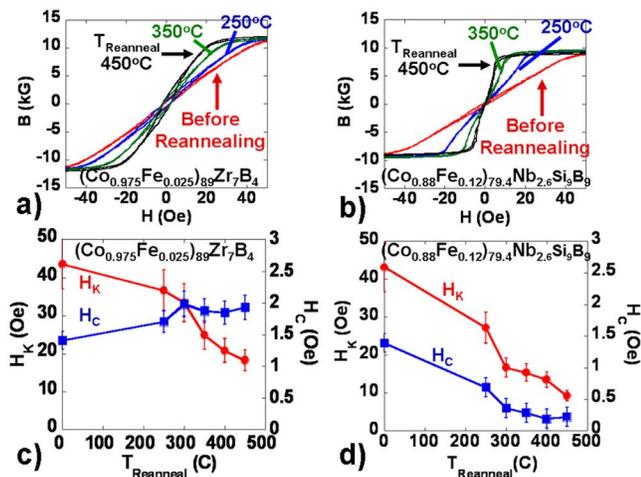

FIG. 2. (Color online) Dynamic ($f = 3$ kHz) B-H loops measured at room temperature for the high field induced anisotropy alloys (a) $(Co_{0.975}Fe_{0.025})_{89}Zr_7B_4$ and (b) $(Co_{0.88}Fe_{0.12})_{79.4}Nb_{2.6}Si_9B_9$ are presented for various longitudinal field reannealing treatments after an initial transverse field crystallization treatment at $T_{anneal} = 540$ °C. (c) and (d) show the corresponding values of H_K and H_C estimated from the B-H loops.
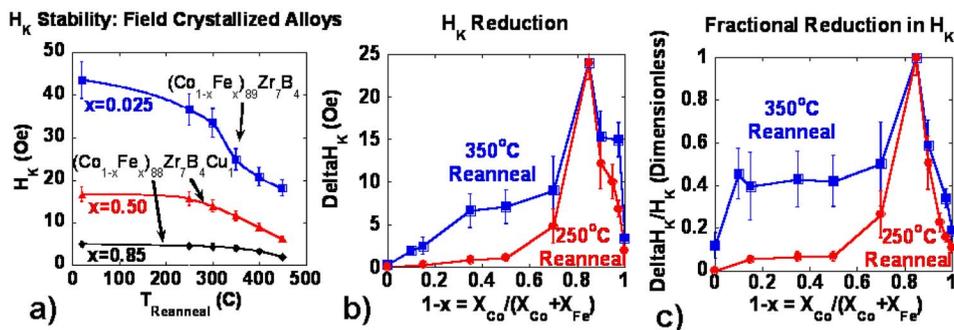
FIG. 3. (Color online) (a) Measured values of H_K at room temperature for several $(Co_{1-x}Fe_x)_{89}Zr_7B_4$ and $(Co_{1-x}Fe_x)_{88}Zr_7B_4Cu_1$ alloys after heating to each reannealing temperature indicated for 1 h with a longitudinal applied field of $H > \sim 50$ Oe and then cooling to room temperature. (b) The reduction in H_K and (c) the fractional reduction in H_K for field crystallized alloys as a function of composition after a longitudinal field reannealing treatment at $T = 250\ °C$ or $T = 350\ °C$.

relatively low temperature stability demonstrated by the $(Co_{0.85}Fe_{0.15})_{89}Zr_7B_4Cu_1$ ($x=0.15$) field crystallized alloy is not understood at this time.

The temperature stability of K_U can provide information about the potential mechanisms responsible for the field induced anisotropy. Further investigation of the temperature stability of K_U is worthwhile in an attempt to clarify the origin of field induced anisotropy in the complex nanocomposites. A comparison between the relative stability of K_U for alloys in which different mechanisms of field induced anisotropy are thought to be dominant could be particularly enlightening.

A final set of experiments demonstrate the importance of applying a magnetic field during crystallization to generate the largest K_U. B-H loops were compared for ribbons crystallized in a transverse field ($T_{anneal}=540\ °C$ for 1 h) with those obtained for ribbons crystallized without a field and then subsequently reannealed in a transverse field (same temperature and time). In Fig. 4(a), B-H loops measured for the zero-field crystallized $(Co_{0.975}Fe_{0.025})_{89}Zr_7B_4$ ribbon are presented and compared to the transverse field crystallized core. No measurable H_K is found after transverse field reannealing of the zero-field crystallized ribbon but there is a large $H_K \sim 43$ Oe ($K_U \sim 22\,000$ ergs/cm^3) for the transverse field crystallized ribbon. Similar results have been obtained for other Co:Fe ratios (for example, $x=0.00$, $x=0.50$, and $x=1.00$) and in all cases transverse field crystallization treatments are more effective than transverse field reannealing of zero-field crystallized ribbons. For the high K_U $(Co_{0.88}Fe_{0.12})_{79.4}Nb_{2.6}Si_9B_9$ alloy a measurable $H_K \sim 22$ Oe (K_U

~ 9000 ergs/cm^3) was induced by transverse field reannealing treatment but it was lower than the $H_K \sim 43$ Oe ($K_U \sim 17\,500$ ergs/cm^3) obtained after transverse field crystallization. We suggest that these observations are likely due to a higher atomic mobility during the early stages of primary crystallization.

Temperature stability of field induced anisotropy, K_U, in amorphous and nanocrystalline/amorphous nanocomposite alloys was investigated. We conclude that (1) field annealing treatments are necessary to investigate the temperature stability of K_U, (2) K_U of field crystallized alloys typically exhibit higher temperature stability than alloys remaining amorphous after field annealing, and (3) larger K_U is obtained for alloys crystallized in a field rather than reannealed in a field after zero-field crystallization. Field crystallization may be required for elevated temperature applications when field induced anisotropy is critical for performance. Experiments examining the temperature stability of K_U for field crystallized alloys deserve further investigation as they may help provide insight into the mechanistic origin of K_U in these complex systems.
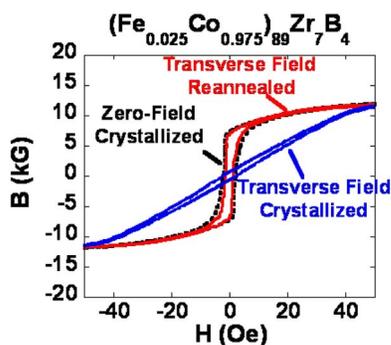
FIG. 4. (Color online) Dynamic B-H loops for a $(Co_{0.975}Fe_{0.025})_{89}Zr_7B_4$ alloy after zero-field crystallization (dashed, black) at $T_{anneal}=540\ °C$ followed by a transverse field reannealing treatment (solid, red) under the same annealing conditions and compared to a transverse field crystallized ribbon at $T_{anneal}=540\ °C$ (solid, blue).

[1] S. Chikazumi, *Physics of Ferromagnetism* (Wiley, New York, 1986).
[2] R. C. O'Handley, *Modern Magnetic Materials: Principles and Applications* (Wiley Interscience, New York, 1999).
[3] G. Herzer, IEEE Trans. Magn. **26**, 1397 (1990).
[4] K. Suzuki, N. Ito, J. S. Garitaonandia, and J. D. Cashion, J. Appl. Phys. **99**, 08F114 (2006).
[5] K. Suzuki and G. Herzer, in *Advanced Magnetic Nanostructures*, edited by D. Sellmyer and R. Skomski (Springer, New York, 2006), pp. 365–401.
[6] K. Suzuki, N. Ito, S. Saranu, U. Herr, A. Michels, and J. S. Garitaonandia, J. Appl. Phys. **103**, 07E730 (2008).
[7] J. McCord and J. Paul, IEEE Trans. Magn. **39**, 2359 (2003).
[8] R. Hasegawa, in *Properties and Applications of Nanocrystalline Alloys from Amorphous Precursors*, edited by B. Idzikowski, P. Svec, and M. Miglierini (Kluwer Academic Publishers, Dordrecht, The Netherlands, 2005), pp. 189–207.
[9] P. R. Ohodnicki, D. E. Laughlin, M. E. McHenry, V. Keylin, and J. Huth, J. Appl. Phys. **104**, 113909 (2009).
[10] P. R. Ohodnicki, Ph.D. thesis, Carnegie Mellon University, 2008.
[11] S. F. Y. Yoshizawa, D. H. Ping, M. Ohnuma, and K. Hono, Scr. Mater. **48**, 863 (2003).
[12] S. F. Y. Yoshizawa, D. H. Ping, M. Ohnuma, and K. Hono, Mater. Sci. Eng., A **375–377**, 207 (2004).
[13] P. R. Ohodnicki, Y. L. Qin, D. E. Laughlin, M. E. McHenry, M. Kodzuka, T. Ohkubo, K. Hono, and M. A. Willard, Acta Mater. **57**, 87 (2009).